Original Research Article

Numerical Study of a Thermal Plume Developing in a Neutral Environment and in Interaction: Application to Fires Problems

Abstract

This study focuses on the mathematical and numerical modelling of how different properties, such as channel length and hot source height, affect the flow of thermal plumes and their interaction with the surrounding environment. Studying the behaviour of a directed thermal plume flow can provide a good visualisation of the control parameters for various applications related to fires and pollutants. To determine the control parameters affecting this flow, it is imperative to initially analyse the flow through a natural convection consisting of a disc-shaped heat source at the inlet of a vertical cylinder using mathematical and numerical methods. The flow in this study is characterised by normal convection, turbulence, steady, two-dimensionality and incompressibility. Numerical results were obtained via computational fluid dynamics analysis, which is based on mathematical flow modelling using the system of Navier–Stokes equations and the finite volume method. The SIMPLE algorithm was used for the velocity–pressure coupling. After introducing the concept of Reynolds averaging and analysis, different RANS turbulence models are presented, particularly two-equation models, using the Ansys Fluent software. Comparison of the different profiles revealed the ideal flow control parameters. An improvement in thermal properties was observedwhen the height of the heat source was h_s = 1.5 cm and the vertical length of the channel was D = 20cm.

Keywords:
Fire simulation, Modified higher, K-epsilon equations, CFD Analysis

INTRODUCTION

Fires in tunnels and buildings produce thermal plumes that emit heat to nearby walls. Heating of the walls caused by thermal radiation leads to the phenomenon of thermosiphon, which interacts with the plume. This study investigates fires as major applications of the turbulent thermal plume's interaction with its surroundings. Many researchers have concentrated on the structure of thermal plumes in a free environment, driven by buoyancy forces. This type of flow has been theoretically and experimentally investigated.

J. Agator[1] examined a thermal plume produced by a spherical calotte heated at a uniform temperature of 500°C. Two flow zones were observed. The plume regularly supplies fresh air during its ascension in the initial zone of pre-turbulence. This zone is characterised by a large temperature gradient and a high velocity. The plume extends to and exports in the second zone of the developed turbulence.

Brahimi et al. [2] conducted an experimental investigation on the configuration of a thermal plume produced by an electrically heated disc at a temperature of 500°C. They observed the presence of the two previously identified zones.

Mahmoud et al.[3] explored how a thermal plume interacts with the thermosiphon surrounding it. The use of the Joule effect to heat a flat disc to 300°C creates a thermal plume. This disc is located at the base of the open-ended vertical cylinder of an adiabatic wall. Aside from the two typical zones discussed in earlier publications about the free plume, Mahmoud et al. also noticed the presence of a third zone close to the temperature source. Thus, they started examining how the thermosiphon affected the heat movement in the column. J. Zinoubi et al. [4] and A. O. M. Mahmoud et al. found another zone [5] in addition to the two zoneformed from the free column. T. Naffouti et al.[6] conducted an experimental study in which they placed a rectangular source heated by a Joule effect at the entrance to an open-ended vertical channel, creating a convection column that caused heating to the adjacent walls. Such heating of the walls by thermal radiation induces a thermosiphon phenomenon that interacts with the column. The results indicated that the turbulent structure of the flow is divided into three areas and that the thermosiphon interferes to reduce the lateral expansion of the column, it activates the upwards flow quickly homogenises the liquid exit the system. Zinoubi et al. [7] focused on the factors affecting the plume–thermosiphon flow, specifically on how the height of the cylinder and its distance from the heat source affect the outcomes. Three separate zones exist inside the plume, with plume contraction being the primary driver in one of these zones. The consistent behaviour of the flow field is caused by the emergence of small, seemingly three-dimensional (3D) structures above this region.

Bouslimi et al. [8] conducted a study on a turbulent thermal plume that was guided by an open-ended vertical cylinder. They experimentally investigated the turbulent structure of the thermal plume produced by a heated disc in a neutral environment. The plume was steered by a vertical cylinder with a thermally insulated wall, set at a distance of 'xc = 1 cm' from the plane of the heated source. The experimental results indicated a change in the flow structure compared with the thermal plume.

A study conducted by Jamil Zinoubi et al. [9] reported that modification of the cylinder spacing and height of the source resulted in a significant shift in the global structure of the plume. Both the flow rate and temperature increased and became uniform during the experiment. The optimal design for increasing the flow rate within the cylinder is h = −5 cm and L = 20 cm. In this setting, the thermosiphon helps the mixing of the fluid and propel it upwards.

To determine how the Prandtl number, length and diameter affect the natural convection heat transfer in a vertical pipe, Ohk S. M. et al. [10] employed both numerical and experimental methods. They conducted a numerical analysis on various pipe D, L and Pr configurations using FLUENT 6.3. Heat transport was hindered by the interactions of thicker thermal boundary layers as the diameter, length and Prandtl values decreased.

Hatem Saafi et al. [11] conducted a study that provided a better understanding of the physicochemical dynamics of tunnel fires in the absence and presence of longitudinal ventilation. Inside a rectangular tunnel with no ventilation system, the production of the thermal plume by the hot source reveals a flow structure separated into three zones. The thermal plume disperses from the source in three distinct locations in the vicinity: a primary exhaust clearing vertically above the source and two secondary exhausts clearing at the source boundaries. The primary plume clearance occurs following a contraction in the second zone. Subsequently, the upwards flow of the plume splits into two directions at the upper portion of the tunnel: an upstream flow called back layering and a downstream flow that borders the ceiling and exits via the free part of the tunnel.

A thermosiphon flow with a thermal plume produced by a hot block centred at the entry of a parallelepiped channel is the subject of an experimental inquiry by T. Naffouti et al. [12]. Only the top wall of the active heater of the rectangular plume is kept at a constant temperature of 300°C. As the channel is increasingly heated, the thermosiphon is intensified, accelerating the upwards flow and facilitating the transfer of energy from a lower- to a higher-temperature zone. This indicates an improvement in both the flow rate and energy absorbed by the fluid.

A study by Zoubir Amine et al. [13] focused on the flow of natural convection in a vertical open channel with a constant heat flux along its walls. Water is used as a medium in both the experiments and computer simulations. The Navier–Stokes equations are solved numerically using a finite difference method (FDM) based on the Boussinesq assumption. The equipment used in the experiment consisted of two heated walls submerged in water. For different wall distances,the paper presents temperature and velocity observations for each of the four possible modified Rayleigh numbers. A numerical benchmark is employed to verify the calculation accuracy of the code. Subsequently, the numerical findings are compared with the experimental findings. Only for low Rayleigh numbers can the algorithm provide a good approximation to the experimental data in terms of the key quantities. With large modified Rayleigh numbers, the flow becomes turbulent and 3D. Thus, over this range of the modified Rayleigh number, two-dimensional (2D) numerical simulations fail to forecast the flow and heat transport.

Saha G. [14] analysed the problem of a stable, laminar, incompressible natural convection flow in an octagon cage. Ra exerted a considerable effect on enclosure convection heat transfer for all Pr values (0.71–50). Pr also affected enclosure natural convection at an Ra > 104.

Fedorov et al. [15] used a channel with vertically parallel plates to study turbulent flow and heat transfer. They utilised the FLUENT computer code. The local Nusselt number distribution and patterns of the fluid flow and heat transmission were also produced by the investigation. The average Nusselt number was shown to have two new correlations.

Bessaih et al.[16] conducted a numerical investigation focused on the 2D, turbulent, natural convection cooling of three hot components that were mounted on a vertical wall. To resolve the equations for the models, the finite volume method (FVM) was employed. It was found that the temperature fields in every part were nearly identical. The temperatures of the components dropped, indicating improved cooling, when the distance between them was increased.

Yun J. H.et al. [17] developed a CFD-based framework to examine the thermal behaviour of reinforced concrete (RC) structures with non-uniform fire damage. To examine a CFD model that predicts fire-induced temperature, RC experimental data were utilised. Subsequently, a CFD model of an RC building frame was created to study column and beam damages under different fire scenarios.

Yang, C., Li, A., et al. [18] developed and validated numerical models to analyse the interaction of thermal plumes from two equal heat sources at varied spacings and the air velocity and temperature distributions of the different spacing ratios. The touching height of the two equal plumes was also examined. The fitting formula for the contacting height is

divided into closely and widely spaced ratios. The touching height of the plumes is minimal at low spacing ratios and grows non-linearly with higher spacing ratios.
Previous literature surveys have highlighted the research gap in the theoretical and numerical simulation of fire applications, specifically in the study of the development of a thermal plume produced by a disc-shaped heat source located at the base of a vertical channel.
The present study aimed to investigate the behaviour of a thermal plume in different regimes evolving in a neutral environment and in its interaction with its surrounding material. The behaviour of the studied flow can provide us with a deeper understanding of the problems of the fire. Thermal plume is produced by a disc-shaped heat source at the entrance of a vertical channel. This study has several differences from previous theoretical studies in terms of the shape of the source as well as the height and shape of the channel. This numerical study was based on computational fluid mechanics. It theoretically and numerically analysed the effect of boundary conditions for the configuration employed and compared it with a free thermal plume.
Another objective of this study was to explore how buoyancy flows occur and what changes happen when the channel length (D) and the hot source higher (h_s) are changed. In this study, the general structure of the flow and how it behaves in terms of heat and motion were first examined. The model under investigation uses the FVM to solve the Navier–Stokes equations for the boundary conditions of the channel. The SIMPLE algorithm was employed to solve the velocity–pressure coupling. Furthermore, the Ansys Fluent software was used to obtain the results. The studied flow is natural convection, turbulent, steady, 2D and incompressible.

1- Theoretical modelling of fire problems

Computational fluid dynamics (CFD) is a computer-aided engineering technology that optimizes cooling energy and heat transmission, fire simulation, and medicinal equipment. The CFD analysis is divided into two major steps: the first step involves theoretical modeling (Figure 1), and the second step involves numerical modeling (Figure 4).

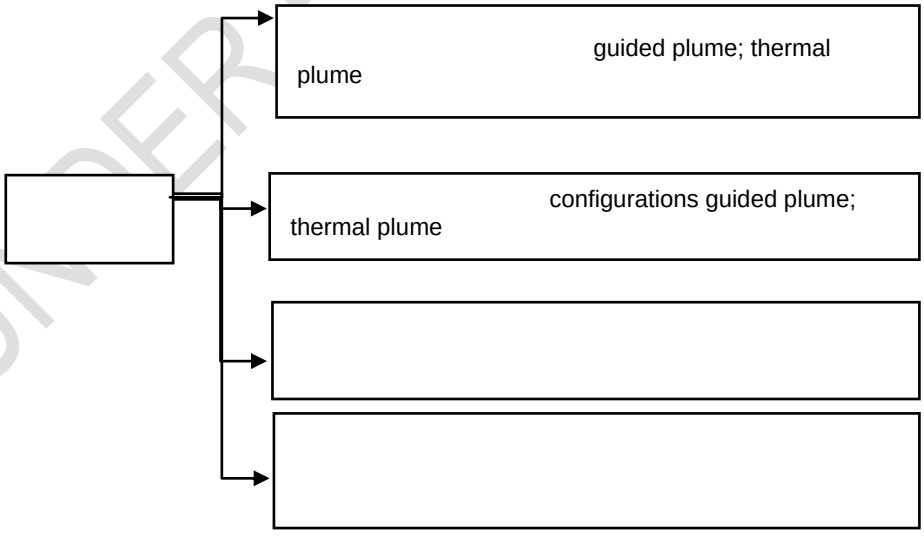

Figure: (1):Steps of the theoretical model of the studied system

1-1 Geometry and boundary conditions

In the study, a vertical channel is utilized, and a circular disc is positioned at the inlet (Figure 2). The heat source is kept at a constant temperature. The source has a temperature of 300°C and two different heights (h_s = 1 and 1.5 cm). The source is placed at the entrance of an open-ended vertical cylinder with a modified height (D = 20, 28, 36 and 45 cm). The first region close to the source is called Z1, the second region is Z2 and the third region is Z3. The wall channel is reheated by thermal radiation emanating from the source. The resulting flow within the vertical channel is a steady, 2D, incompressible, turbulent flow, and the fluid used is air.The boundary conditions are outlined in Table 1.

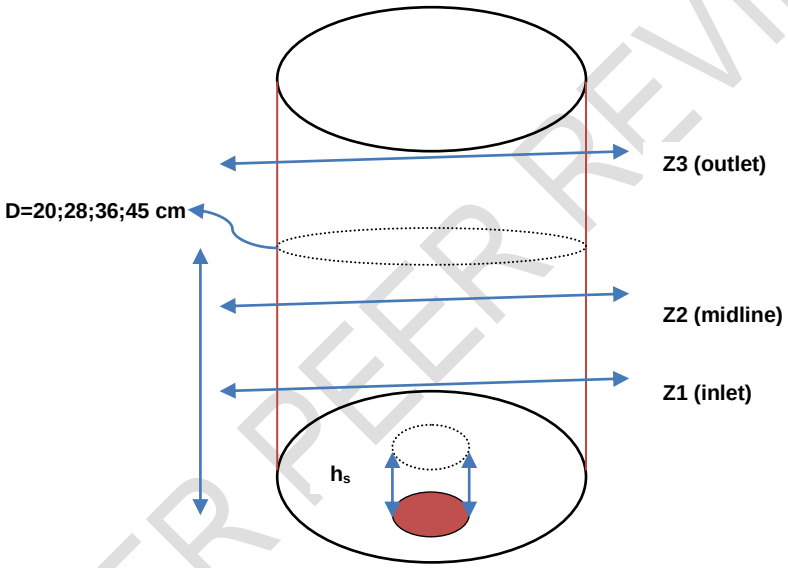

Figure (2): Vertical cylinder with a disc-shaped heat source centered at the channel inlet

Table 1: Boundary conditions for two configurations[22]

Boundary conditionsfor the first configuration	**Boundary conditions the second configuration**
Along the axis of symmetry (r = 0) $\frac{\partial u_r}{\partial r} = \frac{\partial u_z}{\partial r} = \frac{\partial T^*}{\partial r} = 0$	Axis of symmetry (r = 0) $\boldsymbol{\frac{\partial u_r}{\partial r} = \frac{\partial u_z}{\partial r} = \frac{\partial T^*}{\partial r} = 0}$
At the plume source (z=0) $0 \le r \le r_s$ $u_z = u_r = P = 0$, $T^* = 1$ $r > r_s$ $u_r = \frac{\partial u_z}{\partial z} = 0$ $\rho = -\frac{1}{2}u_m^2$ u_m is the average speed at the entry	Inlet condition z=0(at the hot source) $\boldsymbol{0 \le r \le r_s}$ $\boldsymbol{u_z = u_r = P = 0, T^* = 1}$ $\boldsymbol{r_s < r \le a}$ $\boldsymbol{u_r = \frac{\partial u_z}{\partial z} = 0}$ $\boldsymbol{P = -\frac{1}{2}u_m^2}$
At the wall at $z = 1$ $\frac{\partial u_r}{\partial z} = \frac{\partial u_z}{\partial z} = \frac{\partial p}{\partial z} = 0$ $\frac{\partial T*}{\partial z} = 0$	Outlet Condition at $\boldsymbol{z = 1}$ $\boldsymbol{\frac{\partial T^*}{\partial z} = 0 \frac{\partial u_r}{\partial z} = \frac{\partial u_z}{\partial z} = \frac{\partial p}{\partial z} = 0}$
	At the wall at $\boldsymbol{r = r_s}$; $\boldsymbol{u_r = u_z = \frac{\partial p}{\partial z} = 0}$ $\boldsymbol{T^* = \frac{(T_w - T_0)}{(T_s - T_0)}}$

1-2- Study assumptions

The studied flow and fluids are supposed to have the following properties[22, 23]

The studied flow is assumed to:

1- two-dimension
2- Turbulent
3- Steady
4- Axis-symmetric cylindrical coordinates (r,z)

The fluid assumptions are:

1- Newtonian
2- Viscous
3- Transparent
4- The density in the equation of motion is variable the other physical proprieties are constant

2Numerical modelling of fire problems

The second major step in CFD analyses, involving numerical modeling, is outlined in Figure 3 below:

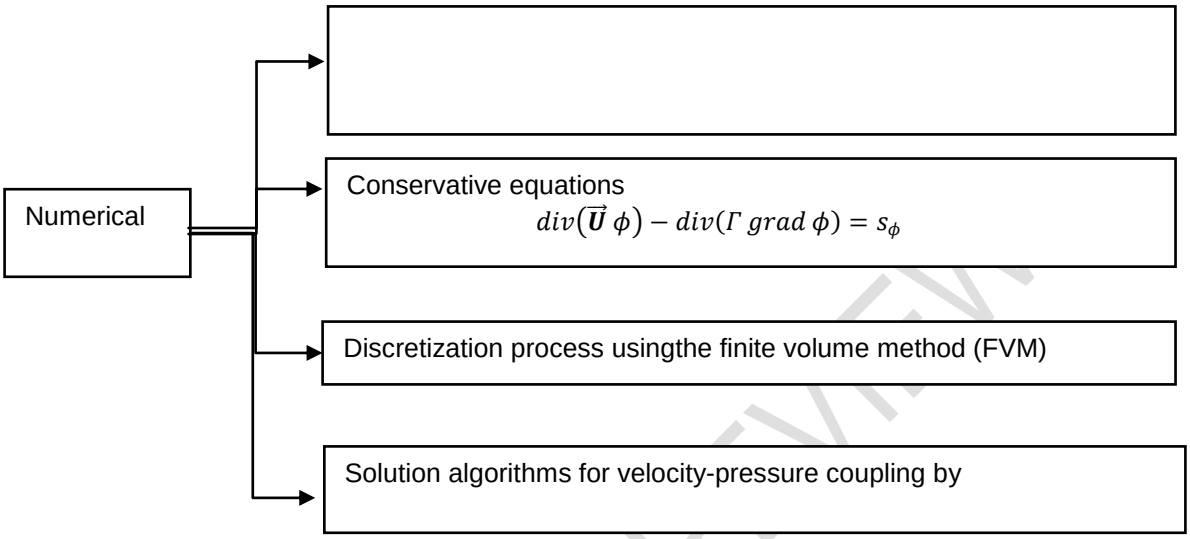

Figure (3):Steps of the numerical model of the studied system

2-1 The studied dimensionless averagesystem

The equations for the conservation of fluid mass (equation 1), momentum and energy govern thermal plumes. Such equations characterise fluid motion in the presence of buoyancy and additional forces. The Navier–Stokes equations(2) and (3) and energy equations (equation 4)are frequently used in the modelling of thermal plumes. Viscous fluids are also modelled using the Navier–Stokes equations. These equations are more complicated than the Boussinesq approximation but simulate thermal plumes better in extremely viscous fluids. The Navier–Stokes equations help explain the vortices of the thermal plume and the interactions with other objects. Thus, mass, momentum and energy conservation principles serve as the basis for the mathematical description of fluid motion[24].

The continuityequation:

$$\frac{1}{R}\frac{\partial}{\partial R}(RU_R) + \frac{\partial}{\partial Z}(U_Z) = 0 \qquad (1)$$

The r-momentumequation:

$$\left(U_R\frac{\partial U_R}{\partial R} + U_Z\frac{\partial U_R}{\partial Z}\right) = -\frac{\partial P}{\partial R} + Pr\frac{\partial}{\partial Z}\left[\left(\frac{\partial U_R}{\partial Z} + \frac{\partial U_Z}{\partial R}\right)\right] + Pr\frac{\partial}{\partial R}\left[2\frac{\partial U_R}{\partial R} - \frac{2}{3}\left(\frac{\partial U_Z}{\partial Z} + \frac{1}{R}\frac{\partial}{\partial R}(RU_R)\right)\right] +$$

$$Pr\frac{2}{R}\left(\frac{\partial U_R}{\partial R} - \frac{U_R}{R}\right) \quad (2)$$

The z-momentumequation:

$$\left(U_R\frac{\partial U_Z}{\partial R} + V_Z\frac{\partial U_Z}{\partial Z}\right) =$$

$$-\frac{\partial P}{\partial Z} + Pr.Ra.T + Pr\,\frac{\partial}{\partial Z}\left[2\frac{\partial U_Z}{\partial Z} - \frac{2}{3}\left(\frac{\partial U_Z}{\partial Z} + \frac{1}{R}\frac{\partial}{\partial R}(RU_R)\right)\right] + +Pr\frac{1}{R}\frac{\partial}{\partial R}\left[R\left(\frac{\partial U_R}{\partial Z} + \frac{\partial U_Z}{\partial R}\right)\right] \quad (3)$$

The equation of energy:

$$\left(U_R \frac{\partial T}{\partial R} + U_Z \frac{\partial T}{\partial Z}\right) = \frac{\partial}{\partial Z}\left(\frac{\partial T}{\partial Z}\right) + \frac{1}{R}\frac{\partial}{\partial R}\left(R\frac{\partial T}{\partial R}\right) + \frac{Ec}{Ra}\left[\frac{1}{Pr}\left(U_Z \frac{\partial P}{\partial Z} + U_R \frac{\partial P}{\partial R}\right) + \Phi_v\right] \quad (4)$$

where $\Phi_v = \left[2\left(\frac{\partial U_Z}{\partial Z}\right)^2 + 2\left(\frac{\partial U_R}{\partial R}\right)^2 + 2\left(\frac{U_R}{R}\right)^2 + \left(\frac{\partial U_Z}{\partial R} + \frac{\partial U_R}{\partial Z}\right)^2 - \frac{2}{3}\left(\frac{\partial U_R}{\partial R} + \frac{\partial U_Z}{\partial Z}\right)^2\right]$

The k-equation:

$$\frac{1}{R}\frac{\partial}{\partial R}\left[R\left((U_R K) - \left(Pr + \frac{\mu_t}{\alpha_k}\right)\frac{\partial K}{\partial R}\right)\right] + \frac{\partial}{\partial Z}\left[(U_z K) - \left(Pr + \frac{\mu_t}{\alpha_k}\right)\frac{\partial K}{\partial z}\right] = -Ra\, Pr\lambda_t \frac{\partial T}{\partial Z} - \varepsilon \quad (5)$$

The ε-equation:

$$\frac{1}{R}\frac{\partial}{\partial R}\left[R\left((U_R \varepsilon) - \left(Pr + \frac{\mu_t}{\alpha_\varepsilon}\right)\frac{\partial \varepsilon}{\partial R}\right)\right] + \frac{\partial}{\partial Z}\left[(U_z \varepsilon) - \left(Pr + \frac{\mu_t}{\alpha_\varepsilon}\right)\frac{\partial \varepsilon}{\partial z}\right] = -\frac{\varepsilon}{k}\left(Ra\, Pr\, C_{\varepsilon 1}\lambda_t \frac{\partial T}{\partial Z} - C_{\varepsilon 2}\varepsilon\right) \quad (6)$$

3. Numerical results and discussion

The fire plume is created by a circular source, as shown in Figure (2). This source at a temperature of 300°C has a modified higher ($\boldsymbol{h_s}$ = 1 and 1.5 cm). The source is placed at the entrance of an open-ended vertical cylinder with a modified higher (D = 20, 28, 36 and 45 cm).

In this section, the heat transfer results of the CFD study are presented, conducted using the Ansys Fluent software.

3.1. Mesh-independent solution results for the CFD simulation

Starting with the conversion of non-dimensional equations into discrete ones using the FVM, a uniform staggered-grid layout is employed. In the pursuit of optimizing the simulation of the studied problem, we conducted a comprehensive analysis of four distinct meshes. The results of this detailed investigation are documented in the Table2.

Table2:Mesh sensitive study

Mesh	Elements	Nodes	Result
Mesh 1	49996	108299	Inconclusive
Mesh 2	74196	162440	Inconclusive
Mesh 3	1038486	2283867	Inconclusive
Optimal Mesh	82375	201018	Excellent

Following a meticulous assessment of each mesh's performance, it was concluded that the mesh with 82375 elements and 201018 nodes yielded outstanding results. Specifically, this mesh demonstrated remarkable symmetry in the evolution of velocity on either side of the cylinder. The curve of the radial component of velocity, plotted at the dimensionless height Z2=0.3, showcased exceptional correlation with model expectations. Results obtained with this mesh exhibited an exceptional correlation with model expectations, reinforcing its relevance for the remainder of the simulation.

3.2Comparison of free plume and fire plume in the channel

This section presents a comparative study based on the experimental results of a free plume conducted by Naffouti et al. [19] and the numerical study of a thermal plume in an open-ended vertical parallelepiped investigated by Jouni et al. [20]. We compare both of these studies with our current work to better understand the research gaps, as highlighted in Table3. This analysis aims to enhance our comprehension of the findings in our study.

Table 3:Comparison of the profile between the configuration, research method and thermal behaviour

Study	Studied flow	Configuration	Study method	Thermal behaviour (Figure5)
Naffoutiet al. [19]	Free thermal plume	Rectangular source surrounded by the atmosphere	Experimental study	Onemaximum of turbulence on the plume axis.
Jouni et al. [20]	Thermal plume in the interaction with its material environment	Rectangular source at the inlet of an open-ended vertical parallelepiped	CFD study using Ansys Fluent software.	One minimum of turbulence on the plume axis, and tow maxima in the both side of the source plume.
Present work	Thermal plume in the interaction with its material environment	Circular source with a modified higher at the entrance of the vertical cylinder with a modified higher.	CFD study using Ansys Fluent software.	One minimum of turbulence on the plume axis, and tow maxima in the both side of the source plume.

While the profiles in Figure (4) of the present study and those of Jouni et al. [20] demonstrate similar behaviors, a subtle distinction is noticeable. This variance can be attributed to the differences in the channel shapes employed in each respective study [21].

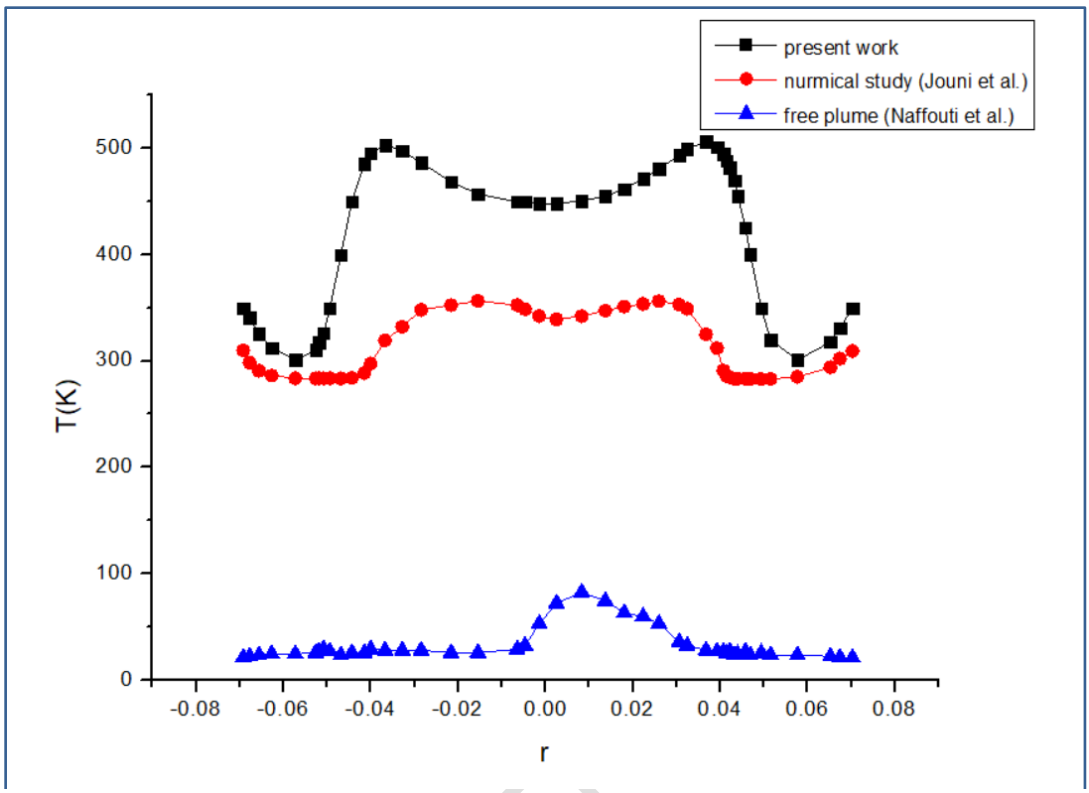

Fig.4. Comparison of free plume and fire plume in the channel

3.3The effect of source geometry

Figure 5 presents the isovalues of the temperature and the velocity for different heat source higher (h_s). These isovalues show the development of fire plume from the channel entry to its exit as well as the region occupied by the plume during its ascension. It also indicates the most turbulent region.
The temperature maxima at the midline of the channel contribute to the formation of two rotating rolls near the hot source. By increasing h_s, Figure (5) demonstrates that the zone in the vicinity of the hot source is increased.

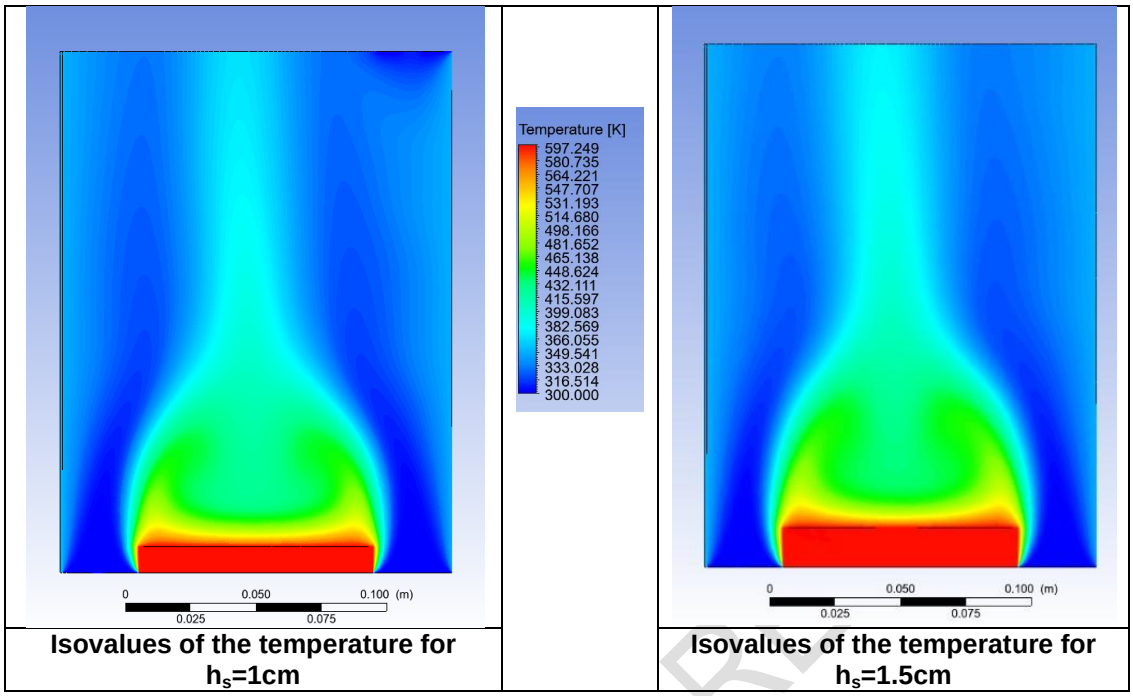

Isovalues of the temperature for h_s=1cm

Isovalues of the temperature for h_s=1.5cm

Isovalues of the velocity h_s=1cm

Isovalues of the velocity h_s=1.5cm

Fig.5. Isovalues of the temperatureand velocity for different heat source higher

The profiles depicted in Figure (6) at the Z1 level exhibit three extrema, with a minimum on the axis and two symmetrical maxima centered at the plume axis. Specifically, as the ambient air comes into contact with the heat source, it undergoes rapid heating, leading to a

significant decrease in density and an increase in viscosity. This process results in a pronounced acceleration of the flow. As the heated air rises, it faces resistance from the surrounding plume air, leading to a persistent swirling of the trapped fluid. This swirling gives rise to two symmetrical rotating rolls around the central axis. Once the air mass accumulates enough energy, it ascends vertically, resulting in a temperature decrease along the plume axis due to the significant influx of fresh external air.

The presented profiles unveil a distinct transverse gradient on each side of the peak. This notable gradient originates from the conversion of ambient air into a heated plume near the heat source. As the source distance increases from the canal entrance, the temperature peaks converge towards the axis, shaping a profile with a singular maximum.

Figure (6) illustrates profiles that demonstrate an enhancement in thermal characteristics within the plume zone when the plume source height is increased ($\boldsymbol{h_s = 1.5\ cm}$). However, it's worth noting that the increased heat source height does not impact the boundary layer flow at the wall.

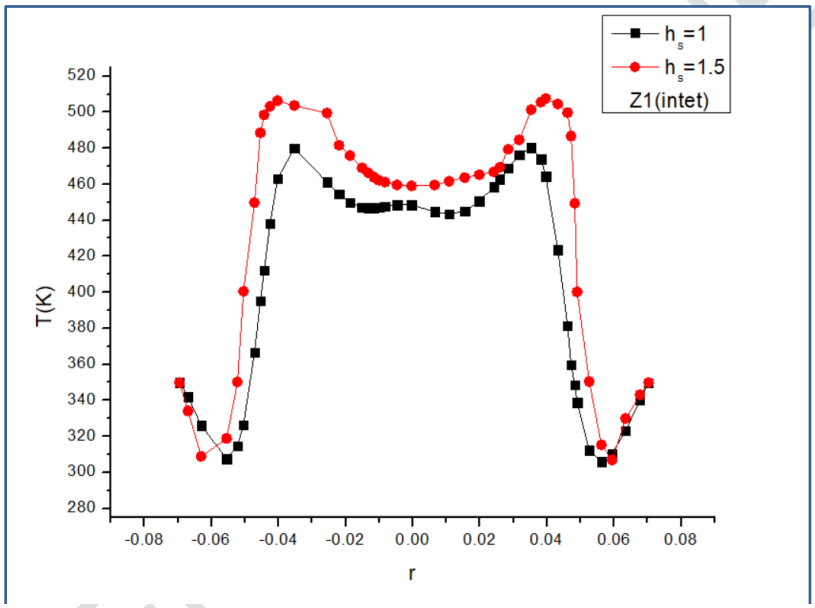

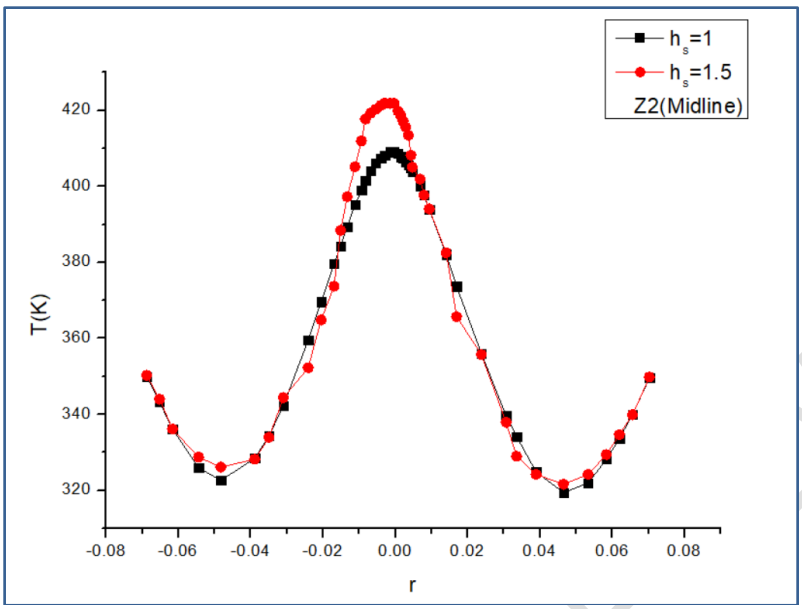

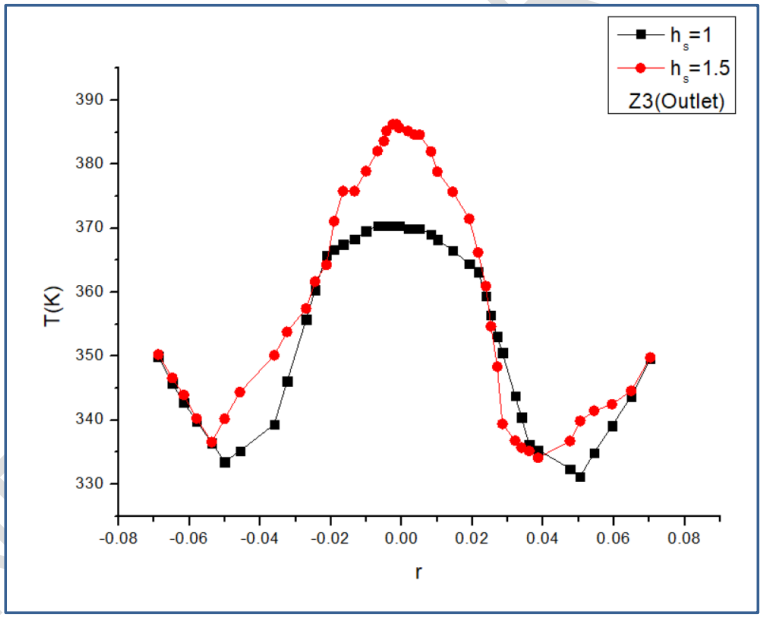

Fig.6. The evolution of the temperature for themodified heat source higher

3.4The effect of channel higher

Figures (7) and 8demonstrate that as the channel length decreases, the temperature increases and the dynamic structure intensifies in the plume zone.

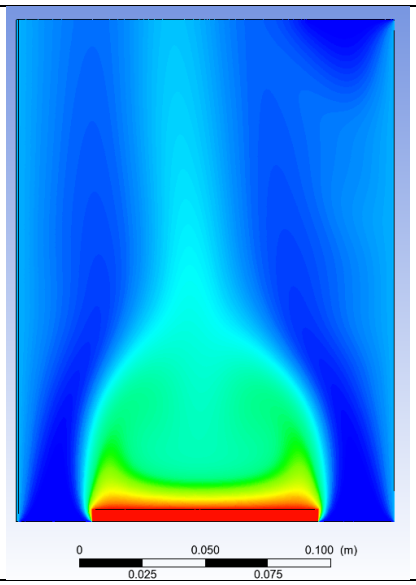

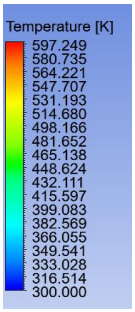

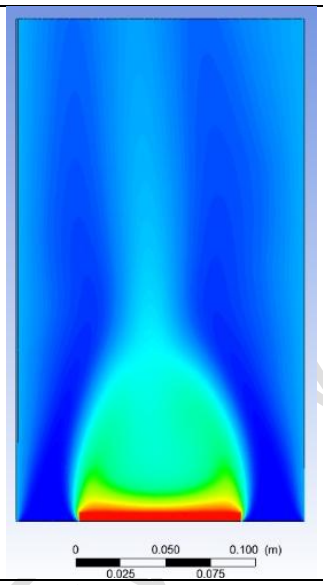

Isovaluesof the temperature for D=20cm

Isovaluesof the temperature for D=28 cm

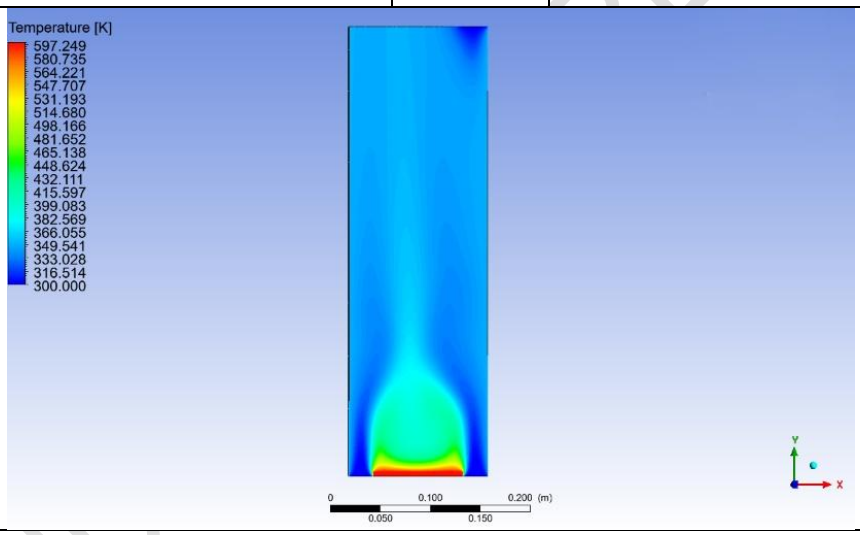

Isovaluesof the temperature for D=45 cm

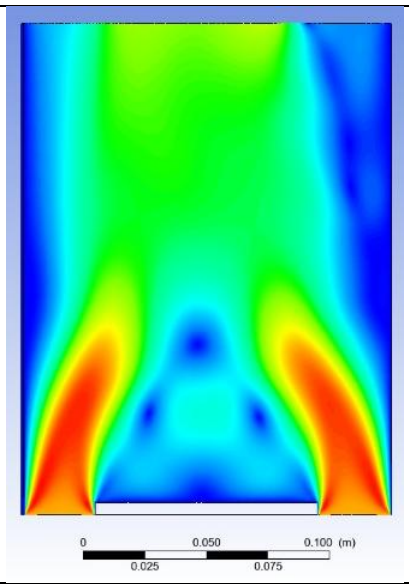

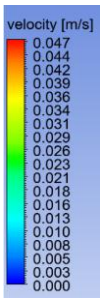

The contour of the velocity D=20 cm

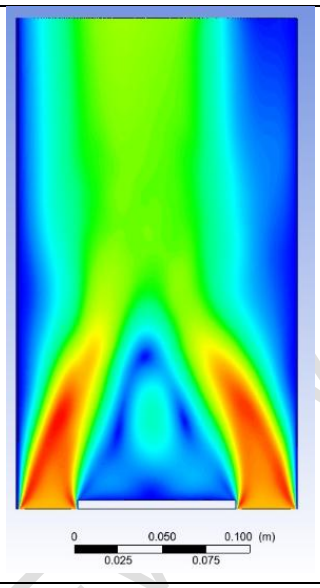

The contour of the velocity D=28 cm

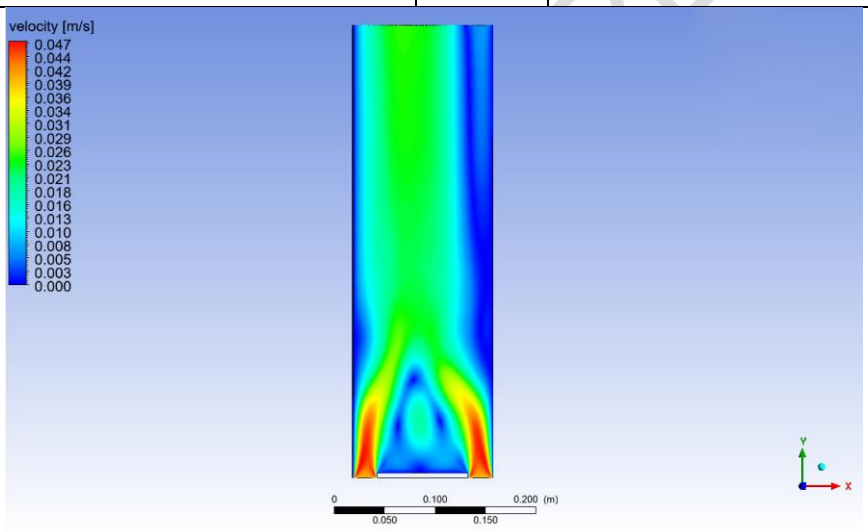

The contour of the velocity D=45 cm

Fig.7. Isovalues of the temperatureand velocity for different channel higher

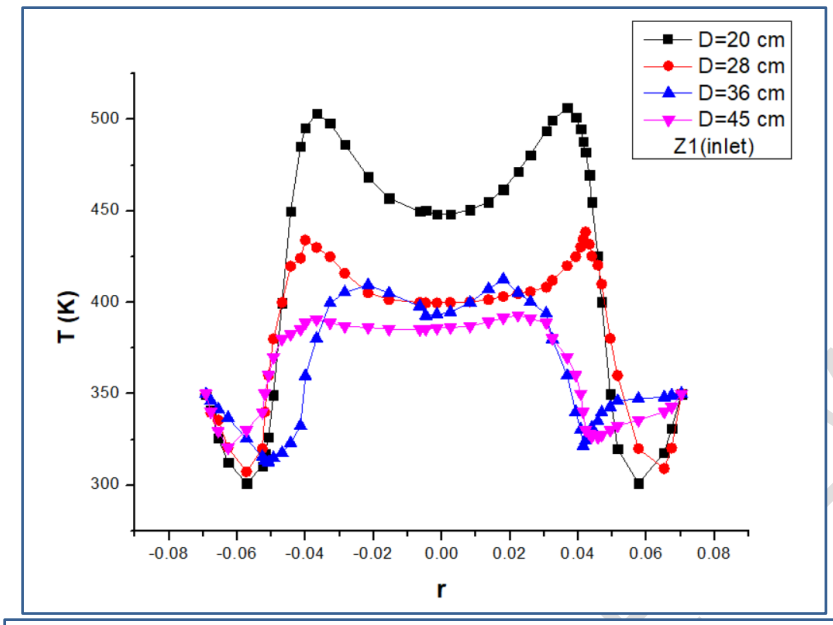
D=20 cm
D=28 cm
D=36 cm
D=45 cm
Z1(inlet)
T (K)
r
500
450
400
350
300
-0.08
-0.06
-0.04
-0.02
0.00
0.02
0.04
0.06
0.08

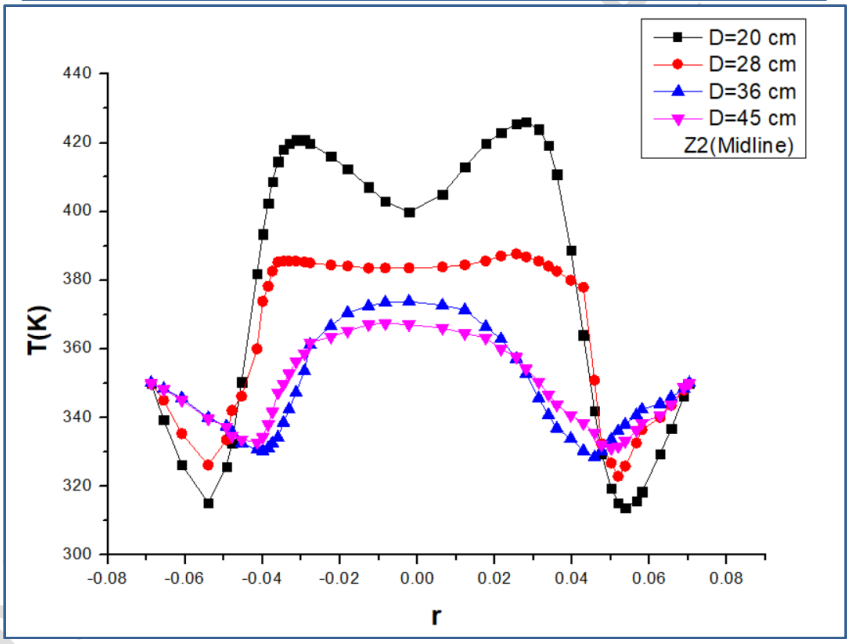
D=20 cm
D=28 cm
D=36 cm
D=45 cm
Z2(Midline)
T(K)
r
440
420
400
380
360
340
320
300
-0.08
-0.06
-0.04
-0.02
0.00
0.02
0.04
0.06
0.08

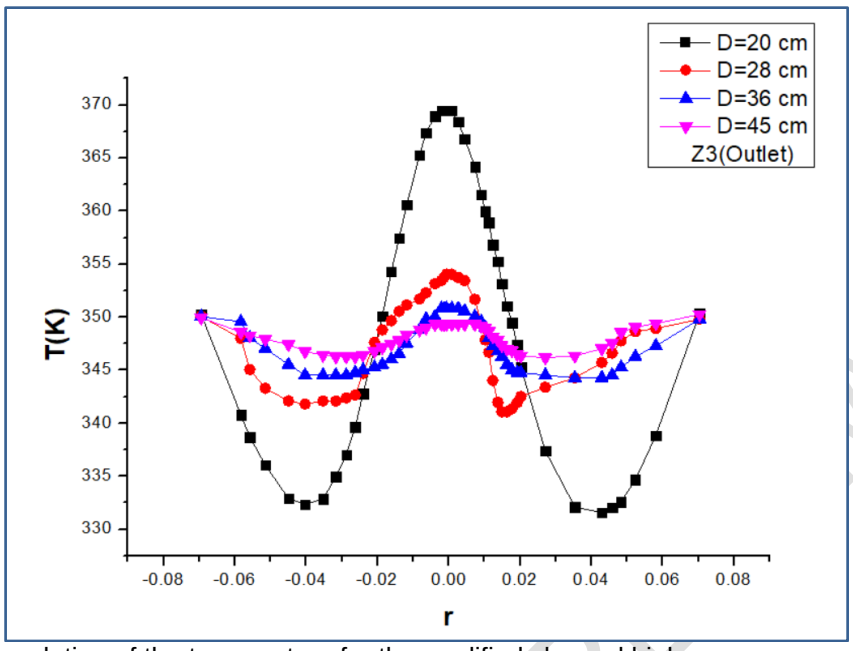

Fig.8. The evolution of the temperature for the modified channel higher

CONCLUSION

This study investigated a turbulent, steady, incompressible, natural convection flow that developed in a vertical channel. Its main objective was to analyse the thermal characteristics of a directed natural thermal plume to enhance its efficiency for various environmental and industrial applications. A simulation was conducted to model the guided natural thermal plume, with the heat source located at the centre of a channel-shaped inlet. The flow was described based on the fundamental physical principles and governing equations that dictate the behavior of fluid flow.To theoretically and numerically simulate the topic of this study, selecting appropriate methodologies was imperative. For this purpose, the k–ε model, FVM and SIMPLE algorithm were employed. The results were obtained using CFD analysis and Ansys Fluent and were then compared with the findings of previous investigations. The comparison of profiles with different values showed that optimisation of the control settings enhanced the efficiency of the thermal flow characteristics.
In this study, the flow under investigation was assumed to be air.However, it is noteworthy that additional fluids need to be considered to more accurately simulate various applications, such as pollutants and fires.
The main findings in this study can concluded by:

- The influence of the hot source on the structure of the fire flow was examined, using two different heights ($h_s = 1\ ;1.5\ cm$).

- The influence of the vertical channel length on the thermal and dynamical behavior was examined, using four different lengths(D=20;28; 36 ; 45 cm).
- The dynamical behavior was depicted in the results along the vertical axis from the cylinder inlet to the outlet using isovalues.
- The thermal behavior was compared for three positions along the vertical cylinder length, at the inlet, midline, and the outlet(Z1, Z2, Z3).

Upon obtaining several results, the optimal control settings for the temperature and velocity contours in the studied flow were identified, i.e., D = 20 cm and h_s = 1.5 cm.

NOMENCLATURE

Γ	diffusion coefficient	Ra	Dimensionless Rayleigh number
$\vec{U}$	Velocity vector	T_∞	Free stream temperature
$U_R,,U_Z$	Dimensionless mean velocity component on (r,,z) direction, respectively	D	Cylinder height
p	Pressure	r_s	Hot source radius
μ_t	Molecular dynamic viscosity	r	Radial coordinate
α_k $\alpha_{\varepsilon,}$	Thermal diffusivity	Z1,Z2,Z3	Inlet, midline, outlet of the vertical cylindrical
ϕ	viscous dissipation function	T_w	The walls temperature
Pr	Dimensionless Prandtl number	T_s	Heat source temperature
T^*	Dimensionless temperature	T_o	Fluid temperature inside the channel
λ_t	Thermal conductivity	h_s	hot source higher
Ec	Dimensionless Eckert number	$u_r,,u_z$	Velocity component on the (r,,z) direction, respectively
a	Channel radius	S_ϕ	Source

REFERENCES

1. Agator, J.M. (1983) “Contribution à l’étude de la structure turbulente d’un panache thermique à symétrieaxiale. Interaction du panache avec son environnementlimité, Thèse. Université de Poitiers.

2. Brahimi, M. (1987) “Structure turbulente des panaches thermique-interaction”, Thèse, Université de Poitiers.

3. Mahmoud, A.O.M., R.B. Maad, A. Belghith (1998) “Interaction d’un écoulement de thermosiphon avec un panache thermique à symétrieaxiale: étude expérimentale”, Rev. Gén. Therm. Vol. 37, pp 385-396.

4. Zinoubi, J., T. Naffouti and R.B. Maad (2011). Temperature Spectra from a Turbulent Free Thermal Plume and in Interaction with its Material Environment, Journal of Applied Fluid Mechanics, (4), pp. 69-76.

5. Mahmoud, A. O. M., Zinoubi, J., Ben Maad, R., & Belghith, A. (2006). Improvement of the Vertical Dispersion of Pollutants Resulting from Chimneys by Thermosiphon Effect. American Journal of Environmental Sciences, 2, 66-73.

6. Naffouti, T., M. Hammami, M. Rebay and R. B. Maad (2009). Experimental Study of a Thermal Plume Evolving in a Confined Environment: Application to Fires Problems. Journal Applied Fluid Mechanics.

7. Zinoubi, J., R.B. Maad, and A. Belghith (2004) “Influence of the vertical source-cylinder spacing on the interaction of thermal plume with a thermosiphon flow: an experimental study”, Experimental Thermal and Fluid Science, Vol. 28, pp 329-336.

8. Bouslimi, J. and L. Dehmani (2005). Experimental investigation of the thermal field of a turbulent plume guided by a cylinder-preliminary results. Experimental Thermal and Fluid Science (29), 477–484.

9. Zinoubi, J., Maad, R. B., & Belghith, A. (2005). Experimental study of the resulting flow of plume–thermosiphon interaction: application to chimney problems. Applied thermal engineering, 25(4), 533-544.

10. Ohk, S. M., & Chung, B. J. (2017). Natural convection heat transfer inside an open vertical pipe: influences of length, diameter and Prandtl number. International Journal of Thermal Sciences, 115, 54-64.

11. Saafi, H., Mahmoud, A. O. M., & Maad, R. B. (2013). Experimental study of the structure of a thermal plume inside a rectangular tunnel. J. of Applied Physics, 4, 18-25.

12. Naffouti, T., Thamri, L., &Zinoubi, J. (2018). On The Experimental Analysis of the Heating Effect of Open Channel on Thermal and Dynamic Characteristics of the Resulting Flow Plume-Thermosiphon. American Journal of Engineering Research, 7(5), 89-106.

13. Zoubir, A., Daverat, C., Xin, S., Giroux-Julien, S., Pabiou, H., &Ménézo, C. (2013). Natural convection in a vertical open-ended channel: comparison between experimental and numerical results. Journal of Energy and Power Engineering, 7, 1265-1276.

14. Saha, G. & Saha, Sumon & Islam, Md. (2010). Natural Convection Heat Transfer within Octagonal Enclosure. *International Journal of Engineering*, *23*(1), 1-10.

15. Fedorov, A. G., &Viskanta, R. (1997). Turbulent natural convection heat transfer in an asymmetrically heated, vertical parallel-plate channel. International Journal of Heat and Mass Transfer, 40(16), 3849-3860.

16. Bessaih, R., & Kadja, M. (2000). Turbulent natural convection cooling of electronic components mounted on a vertical channel. Applied Thermal Engineering, 20(2), 141-154.

17. Yun, J. H., & Jeon, J. (2023). Fire scenario-based damage assessment of ductile reinforced concrete buildings using computational fluid dynamics models. Journal of Building Engineering, 78, 107655.

18. Yang, C., Li, A., Gao, X., & Ren, T. (2020). Interaction of the thermal plumes generated from two heat sources of equal strength in a naturally ventilated space. Journal of Wind Engineering and Industrial Aerodynamics, 198, 104085.

19. Naffouti, T., Zinoubi, J., & Maad, R. B. (2010). Experimental characterization of a free thermal plume and in interaction with its material environment. Applied Thermal Engineering, 30(13), 1632-1643. doi:10.1016/j.applthermaleng.2010.03.021.

20. Jouini, B., Bouterra, M., Vauquelin, O., El Cafsi, M. A., Belghith, A., &Bournot, P. (2009). Thermal plume in a vertical cannal: Effect of the vertical source canal spacing. Paper presented at the CONV-09. Proceedings of International Symposium on Convective Heat and Mass Transfer in Sustainable Energy.

21. Mahmoud, A. M., & Yahya, Z. (2019). Improvement in the Performance of a Solar Hot Air Generator Using a Circular Cone. International Review of Mechanical Engineering, 13(8), 481-492.

22.Ambethkar, V., & Srivastava, M. K. (2017). Numerical solutions of a steady 2-D incompressible flow in a rectangular domain with wall slip boundary conditions using the finite volume method. *Journal of Applied Mathematics and Computational Mechanics*, *16*(2), 5-16.

23. Talluri, Teressa, Tae Hyeong Kim, and Kyoo Jae Shin. "Analysis of a battery pack with a phase change material for the extreme temperature conditions of an electrical vehicle." Energies 13.3 (2020): 507.

24.Han, J. C. (2019). Analytical heat transfer (p. 326). Taylor & Francis.